

OBSERVATION OF MISSING ENERGY ASSOCIATED  
WITH  $\mu^+\mu^-$  PRODUCED IN p-Fe INTERACTIONS\*

A. Diamant-Berger<sup>\*\*</sup>, J.P. Dishaw<sup>\*\*\*</sup>, M. Faessler<sup>†</sup>, J.K. Liu<sup>††</sup>,  
F.S. Merritt<sup>†††</sup>, S.G. Wojcicki

Stanford University, Stanford, CA 94305

B.C. Barish, J.F. Bartlett<sup>§</sup>, A. Bodek<sup>§§</sup>, K.W.B. Merritt, M.H. Shaevitz,  
E.J. Siskind

California Institute of Technology, Pasadena, CA 91125

ABSTRACT

In a study of interactions of 400 GeV protons in a totally absorbing iron calorimeter, we have observed  $\mu^+\mu^-$  pairs associated with a significant amount of missing energy indicative of final state neutrinos. This missing energy is not due to any instrumental effects, nor to any trivial sources like double  $K\bar{K}$  (or  $\pi\pi$ ) decay. Interpreting these data as production of a  $D\bar{D}$  pair followed by a double muonic decay leads to a model dependent estimate of a total production cross section of the order of 6-17  $\mu\text{b}$ .

Submitted to Physical Review Letters

- 
- \* Work supported in part by the Department of Energy under contract DE-AC03-76SF00515 and the National Science Foundation.  
\*\* Permanent address: Department de Physique des Particules, Saclay, France.  
\*\*\* Present address: Intel Corp., Santa Clara, CA 95051.  
† Present address: CERN, Geneva, Switzerland.  
†† Presently with Global Union Bank, Wall Street Plaza, New York 10095.  
††† Present address: University of Chicago, Chicago, IL 60637.  
§ Present address: Fermilab, Batavia, IL 60510.  
§§ Present address: University of Rochester, Rochester, NY 14727.

In an earlier communication,<sup>1)</sup> we have presented evidence for the production of prompt single muons in high energy proton-iron interactions. A natural explanation of this phenomenon is the production and subsequent semileptonic decay of a short-lived heavy hadron, the most likely candidate being a charmed particle (e.g.,  $p + Fe \rightarrow D + \bar{D} + \dots$ ). That same mechanism would also produce events (at a lower rate) with semileptonic decay of both hadrons containing a pair of charged muons and missing energy resulting from the undetected companion neutrinos. In this letter, we present evidence for the observation of such a missing energy in association with hadronically produced  $\mu^+\mu^-$  pairs, and relate it to the rate for our observed single muon signal.<sup>1)</sup>

The experimental apparatus has been described in previous publications<sup>1,2,3)</sup>. Here, we summarize only the salient features. A diffracted 400 GeV proton beam was directed at a sampling iron-scintillator calorimeter that served simultaneously as target and a "live beam dump." The calorimetric information yielded the total hadronic and electromagnetic energy associated with each interaction. The calorimeter, studied extensively with an unbiased sample of proton interactions,<sup>2,4)</sup> gave a linear response over an energy range of 30 to 450 GeV, with the resolution (at the beam intensity used for this experiment) of  $\sigma/E = 0.70/E^{1/2}$  where  $\sigma$  and  $E$  are both expressed in GeV. Furthermore, at the level of 1 part in  $10^4$ , in the unbiased proton interactions, there was no low energy tail (i.e., missing energy) beyond what one expects from a normal Gaussian distribution. There was some high energy tail which was rate dependent and due to pileup<sup>2)</sup>.

The trigger for the  $2\mu$  data reported here selected hadronic interactions that had a final state  $\mu^+$  with  $P_T^+ \gtrsim 0.75$  GeV/c, although the "fuzziness" of the trigger allowed a significant rate of events with  $P_T^+ < 0.75$  GeV/c. The cuts imposed on the hadronic shower and on the quality of the incident proton track were identical to those in reference 2. Thus, a direct comparison of the calorimetry results with those quoted in reference 2 can be performed if the energy of the final state muons is added to the hadronic energy from the calorimeter. To minimize any possible mismeasurements of the muon momenta, we have imposed additional cuts on the muon tracks, requiring the muons to strike the first toroid outside of the central hole, have a minimum of 6 sparks in the toroids and a reasonably good  $\chi^2$  for the fit of their trajectories.

The total data sample that passed all the cuts consisted of 29,895  $\mu^+\mu^-$  and 290  $\mu^\pm\mu^\pm$  events. For each event, we have calculated the missing energy defined by:

$$E_{\text{miss}} = E_{\text{beam}} - E_{\mu^+} - E_{\mu^-} - E_{\text{had}} + 1.3 E_{\text{loss}}$$

where  $E_{\text{beam}}$  is the nominal beam energy (400 GeV),  $E_{\mu^\pm}$  the energy of the  $\mu^\pm$  at the interaction point,  $E_{\text{had}}$  the total hadronic and electromagnetic energy measured in the calorimeter and  $E_{\text{loss}}$  the energy loss of the  $2\mu$ 's via ionization mechanism in the calorimeter. This last term ( $\sim 10$  GeV) corrects for double counting of this energy and the factor of 1.3 allows for the well known inefficiency of the hadronic calorimetry<sup>5)</sup>. The average missing energy calculated in this manner agreed with zero at a level of 1 GeV.

Because of the moderately high  $P_T$  trigger bias, the contribution due to the low mass continuum and the  $\rho$ ,  $\omega$ , and  $\phi$  mesons has been strongly

suppressed in the accepted  $2\mu$  sample. The accepted data contain mainly events from the higher mass continuum and the  $\psi$  decay (which should have no missing energy) and some possible  $D\bar{D}$  events with double muonic events that should be associated with missing energy. The total measured energy distribution of the accepted  $\mu^+\mu^-$  events (Fig. 1) shows good agreement with the sample of unbiased proton interactions in the higher energy half<sup>6)</sup> of the distribution but a significant difference below 360 GeV. Table I illustrates this difference in a quantitative way by comparing the fraction of observed events with either a large missing energy ( $E_{\text{miss}} > 45$  GeV) or a large excess energy ( $E_{\text{miss}} < -45$  GeV) for 3 different data samples.

TABLE I  
 Fraction of events with  $|E_{\text{miss}}| > 45$  GeV (%)

	$E_{\text{miss}} < -45$ GeV	$E_{\text{miss}} > 45$ GeV
Events with no $\mu$ (2)	$0.19 \pm 0.01$	$0.054 \pm 0.006$
$2.6 < M_{\mu\mu} < 3.7$ GeV (3)	$0.16 \pm 0.06$	$0.23 \pm 0.07$
All $\mu^+\mu^-$	$0.26 \pm 0.03$	$0.76 \pm 0.05$

The fraction of events with excess energy is essentially independent of the type of event and can be explained as a Gaussian tail with some possible pileup, but the fraction of missing energy events is significantly higher in the  $2\mu$  sample. As might be expected, this effect is smaller in the 2.6-3.7 GeV region, which is strongly dominated by  $\psi$  production that is unaccompanied by any missing energy. We discuss next the possible known mechanisms that could generate the observed 227 dimuon events with missing energy (ME) above 45 GeV ( $E_{\text{TOT}} < 355$  GeV):

a)  $\tau^+\tau^-$  production followed by muonic decay of both heavy leptons is estimated from the total  $\mu^+\mu^-$  rate at high mass to be less than 1 event.

b) Non-prompt decay of 2 mesons ( $\pi$ 's or K's) produced in the hadron cascade. We empirically set an upper limit of 25% on the fraction of accepted large ME events due to this process from studies of their rate as a function of calorimeter density. However, a much more stringent limit on the possible contribution due to this source is provided by the 5 observed like sign dimuon events with  $ME > 45$  GeV. This number should be a direct measure of the decay background except for the contribution due to production and decay of a single  $K^+K^-$  pair. That contribution has been calculated from the known particle production spectra to yield an additional 6 events based on a rather pessimistic assumption that every primary proton interaction has exactly one  $K^+K^-$  pair. We conclude that no more than 5% of the observed large ME events come from double  $\pi$  or K decays.

c) Catastrophic muon energy loss in the iron toroidal spectrometer. Approximately 1/3 of such events would have been detected by the instrumentation in the first of the six magnets which had acrylic counters after each 20 cm of steel. Comparison of the pulse height in those counters for the large ME events and no ME events (defined here as  $|ME| < 30$  GeV) shows no detectable difference, allowing us to set a limit of 10 events as a possible contribution from that source.

We conclude that the above mechanisms are unlikely to contribute more than 10% of the observed signal. Accordingly, we turn our attention to the most likely explanation, i.e., production and muonic decay of a

pair of charm particles.

To estimate the total charm cross section and to compare  $2\mu$  results with the ones obtained from the  $1\mu$  analysis,<sup>1)</sup> we have assumed that the cross section varies linearly with A and the muonic branching ratio equals 8% and is saturated by the  $K_{\mu\nu}$  and  $K^*_{\mu\nu}$  decay modes.<sup>7)</sup> We have tried the two  $D\bar{D}$  production models which gave good fits to the data discussed in the  $1\mu$  paper:

- 1) a correlated production model described by

$$E \frac{d^3\sigma}{dp^3} = \frac{1}{M^3} e^{-\alpha P_T} (1-x)^\beta e^{-\gamma M/\sqrt{s}}$$

where all the kinematical quantities correspond to the composite  $D\bar{D}$  system that is assumed to decay isotropically, and

- 2) an uncorrelated  $D\bar{D}$  production where each D ( $\bar{D}$ ) is produced independently according to

$$E \frac{d^3\sigma}{dp^3} = e^{-\alpha P_T} (1-x)^\beta$$

With Monte Carlo technique we have calculated the fraction of  $D\bar{D}$  double muonic decays which satisfy our trigger requirement, give  $2\mu$ 's that pass the muon cuts, and yield  $ME > 45$  GeV. Representative results are shown in Table II, where for comparison we have also included the corresponding acceptance (and cross section) from the  $1\mu$  analysis. To extract the cross section from the  $2\mu$  data, we have corrected for small reconstruction inefficiency and subtracted the Gaussian tail (7% from Table I) and contributions from the background processes (10%).

TABLE II

Monte Carlo calculation of acceptance for different models

Model	$\alpha$	$\beta$	$\gamma$	$K/K^*$	$1\mu$ data		$2\mu$ data	
					Acceptance (%)	$\sigma(\mu\text{b})$	Acceptance (%)	$\sigma(\mu\text{b})$
I	1.3	6.0	20.0	1.5	4.6	21.0	0.27	12.3
I	1.3	2.0	20.0	1.5	4.6	20.9	0.47	6.9
I	2.7	6.0	20.0	1.5	3.1	31.1	0.20	16.9
I	1.3	6.0	30.0	1.5	4.1	23.9	0.24	13.9
I	2.2	3.0	14.9	1.5	4.1	23.8	0.39	8.4
I	2.2	3.0	14.9	0.67	3.5	28.0	0.31	10.6
II	2.5	3.0	--	1.5	2.8	35.2	0.22	14.7
II	2.5	5.0	--	1.5	2.4	40.8	0.14	23.8

From these calculations and the comparison of the data with the predicted Monte Carlo distributions, we draw the following conclusions:

- Both models give lower cross sections for the  $2\mu$  data, but the inherent limitations of the experiment (particularly the large background subtractions in the  $1\mu$  analysis) preclude a definitive statement as to the existence of significant discrepancy.
- The uncorrelated  $\overline{D\overline{D}}$  model gives a poor fit to the  $M_{2\mu}$  and  $P_{\mu}$  distributions in the  $2\mu$  data.
- The set of parameters ( $\alpha = 1.3$ ,  $\beta = 6$ ,  $\gamma = 20.0$  and  $K/K^* = 1.5$ ) for Model I appears to be compatible with both sets of the data (see Fig. 2 for comparison with  $2\mu$  distributions) and gives reasonably similar cross section estimates. That model predicts that 6.6% of our accepted  $\mu^+\mu^-$  events originate from  $\overline{D\overline{D}}$  production.
- Within the framework of Model I, adequate agreement with the  $2\mu$  data can be obtained with  $0.7 < \alpha < 2.6$ ,  $3 < \beta < 8$ , and  $10 < \gamma < 30$ . This

range of parameters gives a total cross section estimate from 6 to 17 mb.

Since the total charm production is undoubtedly more complicated than either of the simple models used above, the numbers quoted should be interpreted as giving only a rough estimate of the size of the total cross section. Furthermore, a significant production rate of charmed baryons or unequal  $D^\pm$ ,  $D^0$  branching ratios could generate different cross section estimates for the  $1\mu$  and  $2\mu$  data. Except for this proviso, our data appears difficult to reconcile with the results of Drijard et al.<sup>8)</sup> but seems quite consistent with other positive charm searches.<sup>9)</sup>

Finally, in Fig. 3, we exhibit the ratio of large ME events to all of the observed  $\mu^+\mu^-$  plotted as a function of  $P_T^{\mu^+}$  and  $P_T^{\mu^-}$ . This ratio is insensitive to variation in detection efficiency as a function of  $P_T$ , and the peaking of both of these distributions in the 0.8 - 1.0 GeV/c region, as expected from the charm production hypothesis, provides additional support to our explanation for the observed events.

In summary, we have observed a significant signal of  $\mu^+\mu^-$  events with missing energy in excess of 45 GeV. The most likely explanation of these results is the production and subsequent muonic decay of D mesons, which appears compatible with the data and yields a production cross section that is consistent within errors with the value previously extracted from our single prompt muon signal.

We would like to acknowledge the invaluable contributions of the Stanford and Caltech technical staffs in the design and construction of this apparatus as well as the continuing help of the personnel from the Fermilab Neutrino Lab. One of us (M.F.) would like to thank Max-Kade Foundation for support.



## REFERENCES

- 1) K.W. Brown et al., Phys. Rev. Lett. 43, 410 (1979).
- 2) Limits on the Production of Neutrino-like Particles in Proton-Nucleus Interactions from Calorimetry Measurements, J.P. Dishaw et al., Phys. Lett. (to be published), SLAC PUB-2291.
- 3) Production of  $\psi(3100)$  in 400 GeV Proton Interactions, E.J. Siskind et al., Phys. Rev. (to be published), CALT 68-665.
- 4) The Production of Neutrinos and Neutrino-like Particles in Proton Nucleus Interactions, J.P. Dishaw, Ph.D. thesis, SLAC Report 216.
- 5) A calorimeter will measure a lower energy for a high energy hadron than for an electron or photon of the same energy by about 20-30%. Our calibration allows for this fact and thus the contribution of the ionization loss of the muon to the total "measured" energy in the calorimeter will be higher by this fraction than the actual energy loss. For a more detailed discussion of hadronic calorimetry and a list of appropriate references, see F.J. Sciulli, Photon-collecting Hadron Calorimeters, in Proceedings of the Calorimeter Workshop, Fermilab, May, 1975 (ed. by M. Atac).
- 6) The slight excess (~12 events) of dimuon events at very high energies ( $E > 460$  GeV) is probably due to errors in muon track reconstruction. Because of preponderance of low energy  $\mu$ 's in the accepted data sample, these mistakes will generally give anomalously high muon (and thus total) energy.
- 7) The Semi-leptonic Decays of the D Meson, W. Bacino et al., SLAC PUB-2353 (submitted to Phys. Rev. Letters).

- 8) D. Drijard et al., Phys. Lett. 81B, 250 (1979). One should note, however, the difference in  $\sqrt{s}$  of the 2 experiments: 52.5 GeV vs. 27.5 GeV.
- 9) P. Alibrand et al., Phys. Lett. 74B, 134 (1978); T. Hansl et al., Phys. Lett. 74B, 139 (1978); P.C. Bosetti et al., Phys. Lett. 74B, 143 (1978); A.G. Clark et al., Phys. Lett. 77B, 339 (1978); N. Ushida et al., Lett. al Nuov. Com. 23, 577 (1978).

FIGURE CAPTIONS

- Fig. 1 Total energy distribution for the accepted  $\mu^+\mu^-$  events. The dashed line is a smooth curve corresponding to the observed total energy distribution for an unbiased sample of proton interactions taken simultaneously with the  $2\mu$  data.
- Fig. 2 Comparison of data (solid line) and Monte Carlo predictions (dashed line) for  $P_T^+(a)$ ,  $P_T^-(b)$ ,  $P^+(c)$ ,  $P^-(d)$ , missing energy(e),  $M_{\mu\mu}$  (f).
- Fig. 3 Ratio of number of  $\mu^+\mu^-$  events with large missing energy to all of the observed  $\mu^+\mu^-$  events as a function of  $P_T^+(a)$  and  $P_T^-(b)$ .

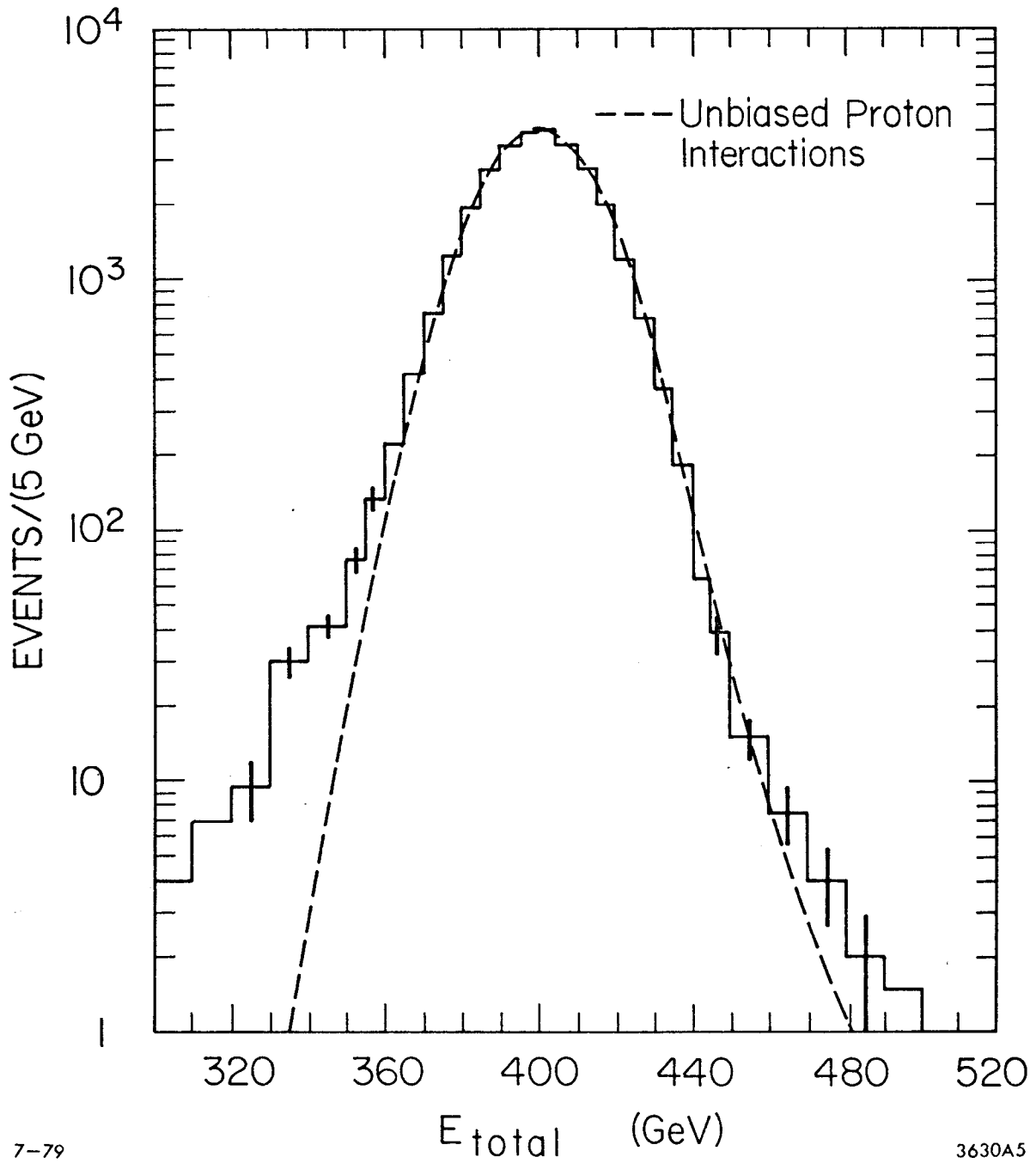


Fig. 1

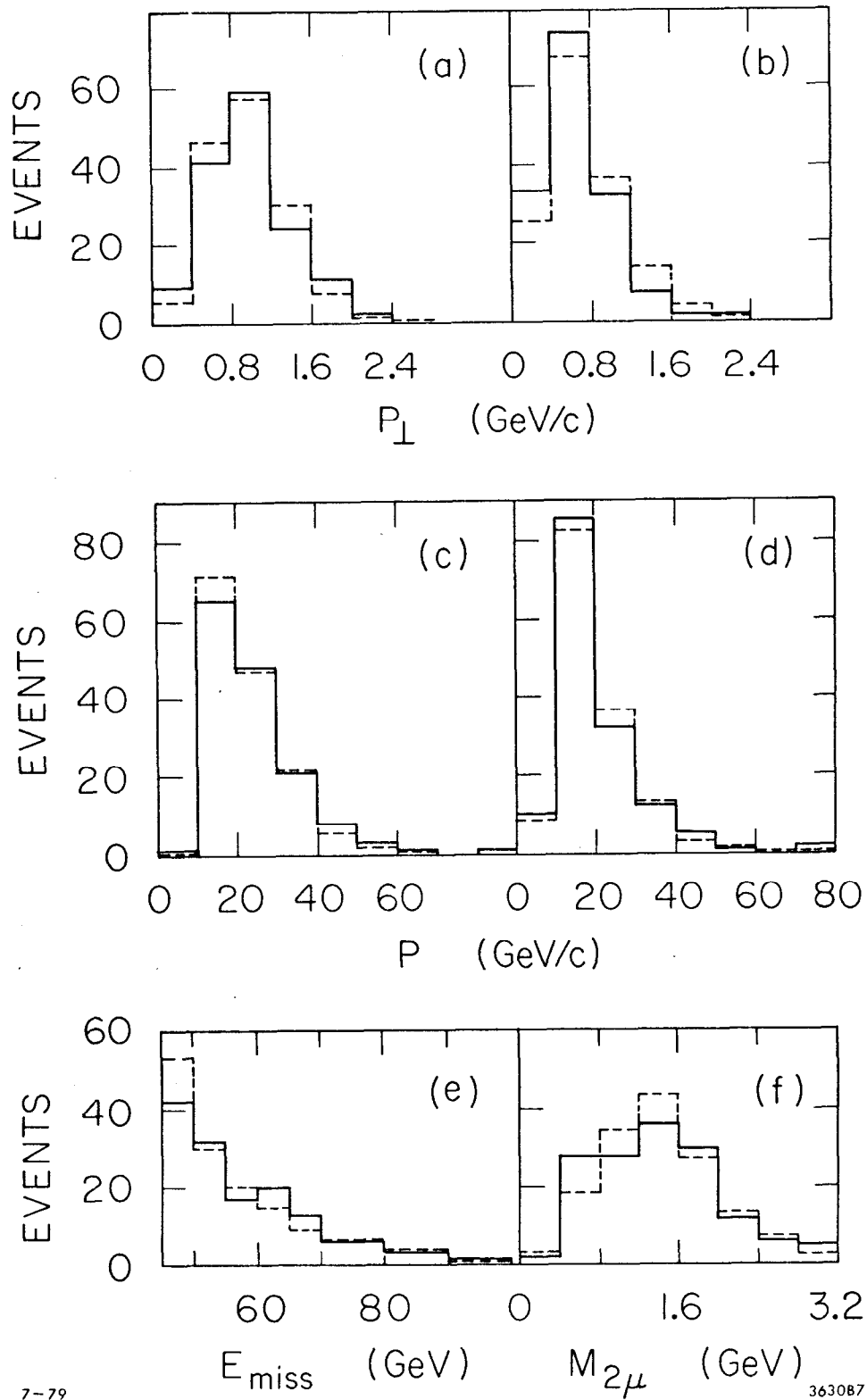


Fig. 2

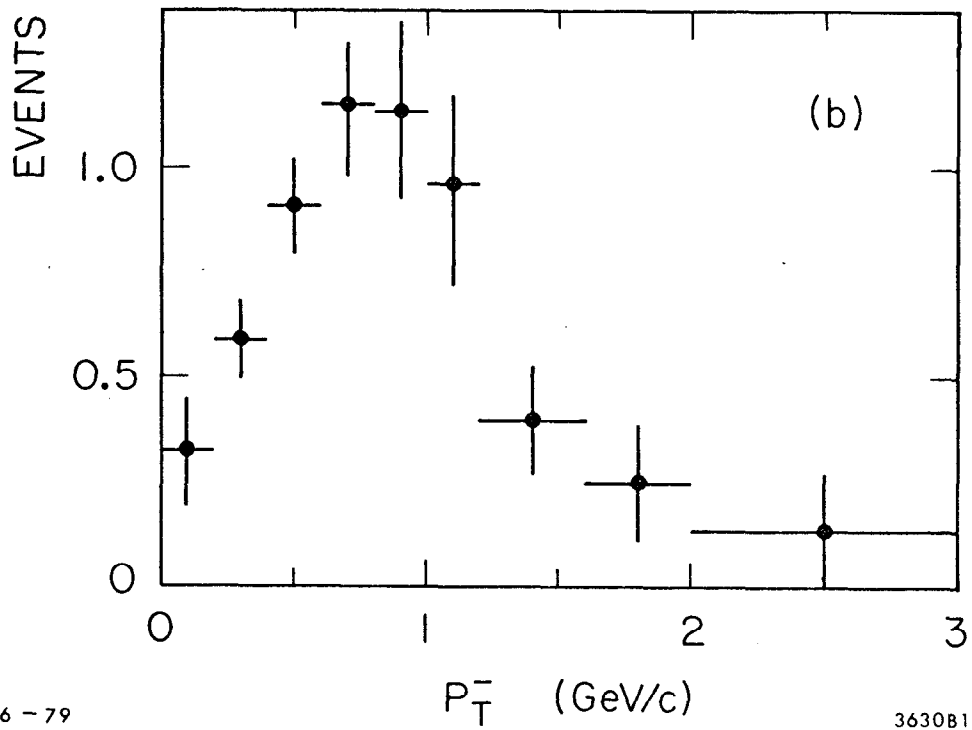
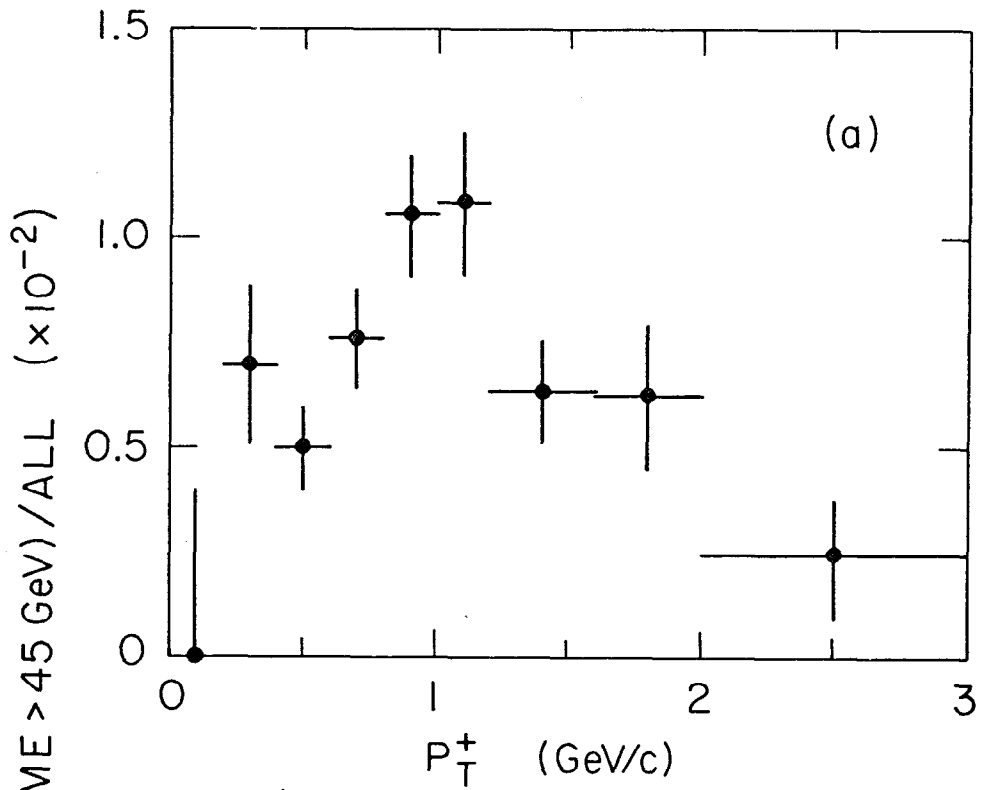


Fig. 3